Current Research in Food Science 7 (2023) 100611

Contents lists available at ScienceDirect

Current Research in Food Science

journal homepage: www.sciencedirect.com/journal/current-research-in-food-science

Thermo-reversible gelation of myofibrillar protein: Relationship between coiled-coil and thermal reversibility

Lingying Zhang [a,b,1], Yanna Zhang [a,b,1], Yue Wang [a,b], Xing Chen [a,b,*]

[a] State Key Laboratory of Food Science and Resources, Jiangnan University, Wuxi, Jiangsu, 214122, China
[b] School of Food Science and Technology, Jiangnan University, Wuxi, Jiangsu, 214122, China

ARTICLE INFO

Keywords:
Myofibrillar protein
Thermo-reversible gel
Coiled-coil
Protein glutaminase
Trifluoroethanol

ABSTRACT

Thermo-reversible gel of myofibrillar protein (MP) can be made by tactics of elaborate deamidation using protein-glutaminase (PG), and this work aimed to disclose the link between thermally reversible gelation of MP and the coiled-coil (CC). Enzymatic deamidation fragmented myofibril filaments and triggered structural reassembly to create small-sized aggregates. The coiling and dissociation of CC structure in the myosin tails is the fundamental structural basis of the PG deamidated MP (DMP) in the dynamic evolution of reversible gelation. After specific inhibition of CC assembly by trifluoroethanol (TFE), the thermo-reversible gel ability of DMP was impaired, which confirmed that the dynamic assembly of CC with temperature response played a key role in the thermo-reversible gelation of DMP. The findings may broaden the molecular basis of natural CC reversible gelation and foster advances for the development of new muscle protein products.

1. Introduction

Thermo-reversible gels are constructed from solutions of natural or synthetic polymers that are capable of melting and reconstituting under temperature stimulation. Thermo-reversible gels not only represent thermally reversible properties, but also show excellent properties such as superb solubility, high water holding capacity, self-healing and membranous ability, thus making them of great interest in food, functional materials and drug delivery applications (Meleties et al., 2021). In the food industries, thermally reversible gels produced from gelatin, curdlan, gellan gum, carrageenan, etc., have played an essential role in the production of jellies, desserts, yogurts, and beverages by virtue of their outstanding 'melting in the mouth' sensation (Aquinas et al., 2021; Du et al., 2016; Khan et al., 2007; Li et al., 2019; Nitta, 2023; Zhou et al., 2012). The oral melting capabilities of thermally reversible gels promote surface lubricity to simulate fat feeling, which implies that when goods require less fat to be added, particular gel design can retain the sensory features of the meal (Hayakawa et al., 2014). In addition, the use of readily meltable or friable gels can enhance the taste, thereby reducing the amount of taste enhancers required, such as salt and sugar (Sala et al., 2010). Recently, several natural proteins have been modified and tuned to trigger thermally reversible gelation behavior. Gel made with krill protein isolate has thermal reversibility during repeated heating/cooling cycles, outstanding gelling capabilities, and a high nutritional profile, allowing it to be employed in food preparation as a food ingredient or nutritional supplement (Wang et al., 2015). Thermally reversible pea protein gels are translucent and have high mechanical qualities, making them a suitable replacement for gelatin in food production scenarios involving low acidic pH settings such as fruits, drinks, and fermented foods (Zhu et al., 2022). By adding dithiothreitol (DTT), egg white lysozyme generated a thermally reversible gel, facilitating cell growth (Yan et al., 2008).

In the field of biomedical materials, a bottom-up approach is often used to design thermally reversible synthetic protein molecules, with many molecular building blocks playing an important role in the process (Prince and Kumacheva, 2019; Wang et al., 2019). The coiled-coil (CC) is one of naturally ubiquitous protein folding and attractive assembly motif made of two or more α-helices entwined together to form a supercoil (Yu, 2002). The CC has excellent reversibly tunable abilities, such as self-assembly and self-healing responding to pH, ionic strength and temperature changes, which make it a viable building block for smart hydrogel creation (Tunn, 2020). As shown in Fig. 1, the primary structure of CC has a repetitive heptapeptide sequence, named heptads $(abcdefg)_n$, where the a and d positions of each heptad are usually

* Corresponding author. State Key Laboratory of Food Science and Resources, Jiangnan University, Wuxi, Jiangsu, 214122, China.
E-mail address: xingchen@jiangnan.edu.cn (X. Chen).
[1] These authors contributed equally to this work.

https://doi.org/10.1016/j.crfs.2023.100611
Received 28 August 2023; Received in revised form 29 September 2023; Accepted 2 October 2023
Available online 5 October 2023

non-polar hydrophobic amino acid residues, such as leucine, isoleucine, valine, etc., while the e and g positions are usually polar charged amino acid residues, such as lysine, glutamate, etc., forming ionic interactions (Tunn, 2020; Xu et al., 2005). CC performs physical cross-linking, which is caused by reversible intermolecular interactions between helical chains, and creates oligomers, allowing CC-containing proteins to form fibrous hydrogels with a controlled gelation process (Dong et al., 2008). Among them, physical crosslinking is mainly mediated by molecule entanglement or non-covalent interactions such as hydrogen bonding, van der Waals forces, electrostatic or hydrophobic contacts, and so on (Wang and Heilshorn, 2015). Thermally reversible hydrogels with a single convoluted helical protein structural domain can be stabilized by molecular entanglement between protein nanofibers to form porous matrices capable of binding hydrophobic small molecules of curcumin and used as sustained release carriers to control drug release at physiological temperatures via gel-sol transition behavior (Hill et al., 2019). At physiological pH and salt conditions, a coiled-coil (CC) peptide-based hydrogel with thermo-reversible gelling capacity can support the growth of mouse fibroblasts, providing molecularly simple tissue engineering applications and biodegradable alternatives to polymer-based systems for biomedical applications (Dexter et al., 2017). This demonstrates that designing and manufacturing CC-based nanofibers might be a viable technique for producing thermally reversible gels from natural proteins.

CC structures are naturally presented in MP (Myofibrillar protein). Muscle myofibrils are mostly formed of myosin thick filaments, and the whole supramolecular architecture is around 1.6 m long and 13–18 nm in backbone diameter, and is constructed by 250–300 myosin molecules organized tail-to-tail via the myosin rod domain (Liu et al., 2017; Rahmani et al., 2021). The myosin rod domain is typical of the CC structure, implying that myosin thick filament is rich in CC nanofibrillar structures. Recently, thermally reversible gels from myofibrillar protein were pioneerly reported by our group (Zhang et al., 2022). After more than five cycles of heating and cooling, gel demonstrates thermal reversibility. The gels were prepared by heating 2.5% protein solutions treated with PG deamidation. And it displayed a perforated lamellar microstructure with good water holding capacity over 95%. However, the fundamental principles responsible for the thermo-reversible behavior of mildly deamidated MP, herein referring to the connections with CC, was unresolved. Trifluorethanol (TFE) was discovered as cosolvents that have a prominent effect on the CC structure of peptides and proteins (Vymetal et al., 2016). TFE can geometry adaptively penetrate the hydrophobic core of CC and disrupt tertiary or quaternary archtectures stabilized by hydrophobic contacts while stabilizing secondary structures, which means TFE can specifically inhibit the CC formation whilst stabilizing the individual helix, hence it is used as a specific probe to determine the functional properties of CC (Haider et al., 2018; Othon et al., 2009). The aim of the current work was to uncover the mechanism by connecting CC to the thermally reversible gelation of deamidated MP. The study on thermally reversible gels of MP would open up a wide range of innovative and beneficial applications of muscle proteins in the food industry.

2. Materials and methods

2.1. Materials

Chicken breast meat obtained from chickens weighing an average of 2.5–3.0 kg at 42 days of age and purchased within 48 h postmortem from Sushi Food Co. (Jiangsu, China). After pre-treatment of the chicken breasts to remove some of the visible tendons, the breasts are vacuum-packed and stored in a refrigerator at −20 °C for use within 7 days. To ensure that variances between the original meat samples were kept to a minimum, chicken breasts with identical drip loss (2%) were selected for usage. Protein-glutaminase (PG) (Amano 500, 500 U/g) was generously donated by Amano Enzyme Manufacturing, Ltd. Shanghai Branch (Shanghai, China). Sodium chloride (NaCl, GR), ethylenediaminetetraacetic acid disodium salt (EDTA-2Na, AR), tris(hydroxymethyl)-aminomethane (TRIS, AR) were attained from Sinopharm Chemical Reagent Co., Ltd. (Shanghai, China). Other chemical reagents were at least of analytical grade and bought from Sigma-Aldrich (MO, USA).

2.2. Preparation of MP

The extraction of chicken breast myofibrillar protein followed our previous procedure with slight modifications (Chen et al., 2016a, 2016b; Ito et al., 2003). Briefly, the meat was minced and rinsed with various concentrations of Tris buffer (5–100 mM NaCl, 5 mM EDTA, and 5 mM Tris, pH 7.2). Following that, the myofibril paste was suspended in twice the volume of 10 mmol/L phosphate buffer (PBS, pH 7.0) and homogenized using the ULTRA-TURRAX (T25 digital, IKA, Germany; 8000 rpm, 3 min). The myofibril suspensions ultimately obtained were regarded as MP. MP was stored in a refrigerator (4 °C) and used within 3 days.

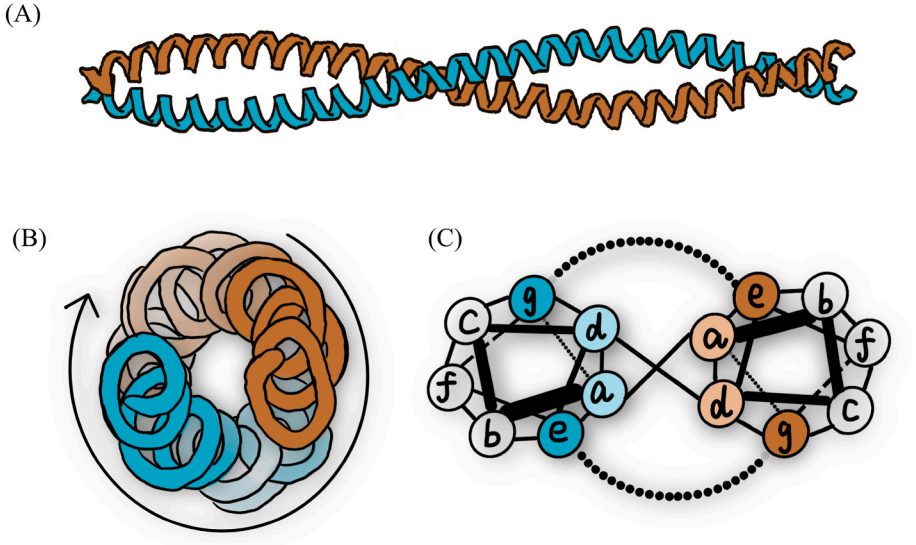

Fig. 1. Schematic drawing of coiled-coil structure. (A) Side view; (B) Top view; (C) Cross-section view shows repetitive heptapeptide sequence heptads $(abcdefg)_n$, with frequently observed hydrophobic amino acids on a and d position.

2.3. Deamidation of MP by PG

The deamidation of MP was performed as previously described (Fu et al., 2022; Zhang et al., 2022). MP (25 g/L, pH 7.0) was treated with PG (16 U/g protein) at 37 °C for 12 h. Afterward, samples were moved to an ice slurry bath (~4 °C) promptly with the purpose of deactivating PG.

2.4. Preparation of thermo-reversible gels

DMP samples were subjected to following cycle of heating and cooling program for gelation: the sample was heated at 90 °C for 10 min, after which the sample was cooled down to 4 °C and the temperature was maintained at 4 °C for 2 h. In the TFE-treated groups, trifluoroethanol (14, 28, 42, 56 mol/g protein) was added to the DMP samples at various concentrations and well mixed before subjecting them to the same treatment conditions. To make salt soluble myofibrillar protein (SMP), an appropriate amount of MP was used to increase the protein content to 25 g/L with 0.6 mol/L NaCl solution, and the same process was utilized to obtain thermal gel. The formed gels were placed at 4 °C for further analysis.

2.5. Atomic force microscopy (AFM)

As previously mentioned, atomic force microscopy (AFM) was used to examine the microscopic morphology of MP and DMP (Chen et al., 2016b; Liu et al., 2021). The linear scanning rate was set at 1 Hz, with 512 samples per line as the scan resolution. Exactly 10 μL of the sample (0.01 g/L) was cast on clean silicon wafers and was allowed to dry in ambient air for 12 h before being exposed to AFM analysis by using tapping mode of Dimension FastScan AFM (Brook, Germany) under atmospheric pressure at 25 °C. All height images were handled with "flatten" function using the Nanoscope Analysis software (Version 1.9) prior to analysis. The height differences, root mean square of roughness (Rq) and average roughness value (Ra) and three-dimensional structures were examined using the "section", "roughness" and "3D image" functions, respectively in the Nanoscope Analysis software (NanoScope v 5.30r3, Veeco, USA).

2.6. Rheological properties

The rheological properties of the thermo-reversible gels were monitored on a DHR-3 rheometer (TA Instruments, DE, USA). A parallel plate with a diameter of 40 mm and a gap of 1 mm was selected. The measurements are specified in the following.

To track the evolution of storage modulus (G′) throughout two cycles of heating-cooling process, a temperature sweep including phases of heating from 25 °C to 90 °C, temperature holding at 90 °C, and follow-up chilling to 4 °C was examined. The angular frequency and strain amplitude are set as 1 Hz and 2%, respectively.

2.7. DMP gelation in comparison to TFE-treated DMP

2.7.1. Gel morphologies

The morphologies of DMP gel and DMP + TFE gel was visualized by scanning electron microscope (SEM) and compared. The gel samples were fixed in 2.5% glutaraldehyde for 2 h and then freeze-dried. The lyophilised protein gels were fixed to the sample stage with conductive adhesive. After gold spraying of the surface, the microscopic morphology was observed using a SEM (FEI quanta FEG 450) under an accelerating voltage of 20 kV.

2.7.2. Individual helix and CC contents

Helical conformation changes of DMP and TFE-treated DMP during one cycle of heating and cooling process were monitored by Circular dichroism (CD) using Chirascan V100 (Applied Photophysics Ltd., UK.). Scan rates and time constants were set to provide enough reaction time while maintaining a good signal-to-noise ratio. At a scanning speed of 20 nm/min, samples were scanned from 190 to 260 nm. Spectra were collected in a 1 mm quartz cuvette at 25 °C. The mean residue ellipticity (MRE, θ) indicating the content of α-helix was calculated from ellipticity values (θ) as follows (Gunasekar et al., 2009):

$$(\mathrm{MRE},\theta)=\frac{\theta}{10\times protein\ concentration\times path\ length\times residue\ number} \quad (1)$$

The α-helical conformation state (individual helix or helical CC) in MP and DMP was evaluated by calculating the ratios of the MRE at 208 and 222 nm ($\theta_{222}/\theta_{208}$). In numerous proteins, $\theta_{222}/\theta_{208}$ has been utilized as an indication to determine the existence of CC. (Choy et al., 2003). The parameters of the temperature scanning experiment were set according to previous studies (Zhang et al., 2022).

2.8. Statistical analysis

All experiments were independently repeated more than three batches. All experimental results are expressed as mean ± standard deviations. Data were plotted using Origin 2022 software. Statistical analysis of the data was performed using IBM SPSS 20.0 software, using single-factor The data were analysed using IBM SPSS 20.0 software, using single-factor ANOVA (Duncan's method) and were considered statistically significantly different at p-values$<$0.05.

3. Results and discussion

3.1. Morphology

As shown in Fig. 2A, a typically intact myofibril structure was observed in the MP solution with filamentous in shape, which is in agreement with the AFM microstructure of rabbit skeletal muscle myofibrils (Yoshikawa et al., 1999) and chicken breast myofibrillar protein (Chen et al., 2016b; Fu et al., 2022) observed previously. After PG deamidation, the disruption of the originally intact filamentous structure was evident in the AFM diagram, with the appearance of myosin-like species, due to the dissociation of myofibrils Fig. 2B. This was consistent with our previous findings, which revealed that PG deamidating caused myofibrils to break and the release of sub-filaments, sprout-like myosin, monomer actin, and their oligomers (Zhang et al., 2022). Also, by profiling the height map analysis revealed a decrease in the height of the particles, it indicated a decrease in the height of the particles.

3.2. Gel appearance and thermo-reversibility

Trifluoroethanol (TFE) is a frequent co-solvent used in peptide and protein experiments, and it has a considerable influence on the CC structure of peptides and proteins (Vymetal et al., 2016). According to relevant research, TFE stabilizes secondary structures and disrupts tertiary or quaternary interactions stabilized by hydrophobic interactions or quaternary interactions (Othon et al., 2009). We confirmed the function of CC in DMP thermo-reversible gel formation by targeting disrupting CC formation with TFE. To investigate if TFE disturbs native MP's gelation (typically known as thermally irreversible gel), salt-soluble myofibrillar protein (SMP) solution was prepared as one of the controls. Native MP is soluble in high ionic strength solutions and its gelation is characterized primarily by covalent cross-linking at the head of myosin when heated and electrostatic cross-linking at the tail. Salt ions can also attach to oppositely charged amino acid side chains in proteins, breaking ionic connections and improving protein interactions (Gong et al., 2022).

After heating, the MP solution showed flocculent aggregates with a clear aqueous phase (Fig. 3A), which did not change considerably when the added TFE concentration rose, and there was no evident change upon cooling, all samples still showed non-uniform aggregates. The

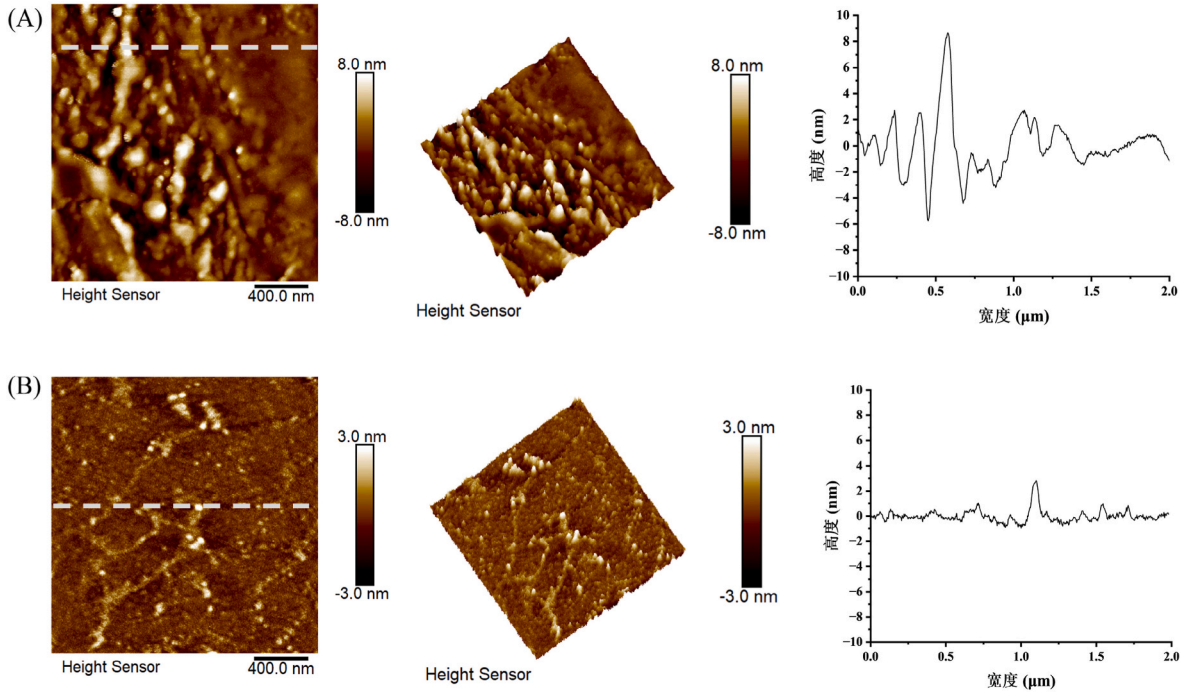

Fig. 2. Representative atomic force microscopy (AFM) images of MP (A) and PG deamidated MPs for (B). The cross-section images correspond to the section in the 2D image are section analyses (height) along the corresponding white dashed lines.

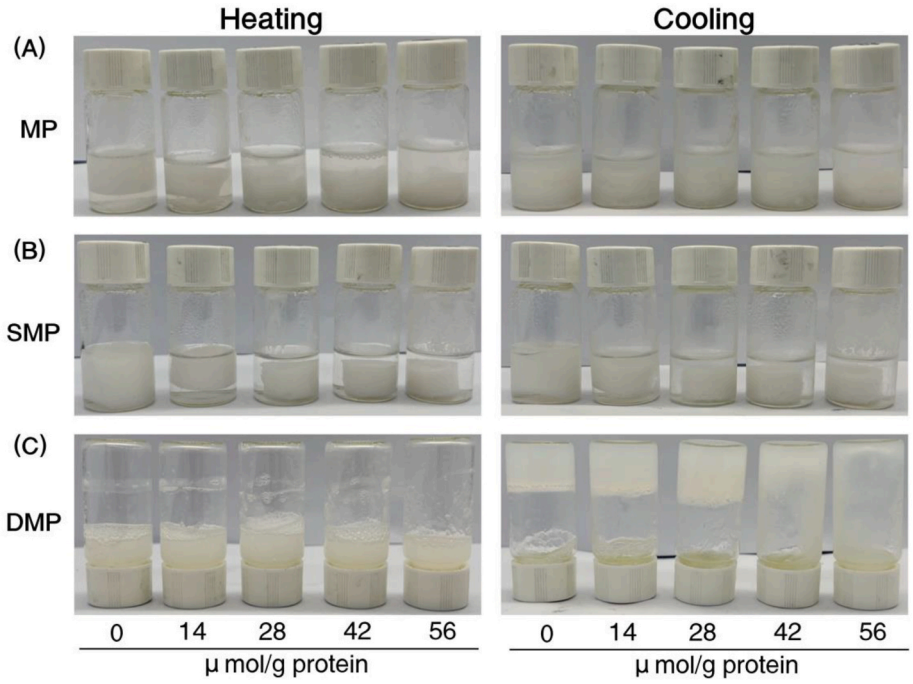

Fig. 3. Effects of TFE addition (0, 14, 28, 42, 56 μmol/g protein) on the colloidal state of (A) MP: Myofibrillar protein; (B) SMP: Salt-soluble myofibrillar protein; (C) DMP: Deamidated myofibrillar protein upon heating and cooling process.

flocculent aggregates were loosely dispersed in the aqueous solution following minor shaking. The SMP solution formed a gel after heating, with a slight amount of water loss, and the gel network did not alter as the temperature dropped further, demonstrating a typical thermally irreversible gelation phenomena (Fig. 3B). It is expected as the SMP had desirable protein solubility and the protein structure unfolds at 0.6 M ionic strength, the interior amino acid side chains exposed to encourage the formation of disulfide bonds. Simultaneously, the electrostatic repulsion among protein molecules is lessened, making them sensitive to denaturation and excessive aggregation, resulting in the formation of a stable three-dimensional network and improved gel characteristics (Gong et al., 2022). The addition of TFE led to a tighter and stronger gel network in SMP which showed less susceptibility to be damaged by external forces (Fig. 3B). The water loss of the gel network gradually elevated with the increase in TFE concentration. This is probably due to the fact that TFE molecules can aggregate around protein molecules,

which not only prevents water molecules from approaching and forming hydrogen bonds with the protein, but also provides a lower dielectric constant that is more conducive to stabilize the protein backbones (Guo and Mei, 2013). As a result, the water loss from the gel exacerbated while the strength of the gel network enhanced. As shown in Fig. 3C, the DMP solution displayed a flowable suspensions upon heating but transformed into a gel after cooling, which agrees with our previous findings (Zhang et al., 2022). When heated, the DMP with TFE did not affect the colloidal state of DMP after heating but it gradually impaired the cold induced gel formation as its dosage increased. Especially at concentrations above 28 μmol/g protein, TFE inhibited the gelation of DMP and induced flowable suspensions (Fig. 3C). There results suggested that TFE pronouncedly suppressed the cold induced gelation of DMP but scarcely affected thermally induced gelation of MP or SMP. CC is a reversible assembly which can be physically coiled during cooling, and TFE specifically disrupts the CC, it is thus deduced that the formation of reversible gels of DMP upon cooling is closely related to CC. Once CC assembly was prohibited during cooling, the cold induced gelation of DMP would be prevented.

To further inspect this deduction, the effects of TFE on the reversibility of DMP gelation was determined. Fig. 4 shows the gelation of samples from the TFE treated DMP group after repeated heating and cooling. Without TFE, DMP exhibited obvious thermo-reversible gel characteristics which can sustain five heating-cooling cycles in consistent with previous observation (Zhang et al., 2022). TFE addition can gradually damage the reversibility of DMP gelation in a dose dependent manner (Fig. 4). DMP with the addition of 28 μmol/g of TFE showed a weak gel strength at the third cycle of cooling, a slow onset of flow on inversion and a gradual weakening of the cold gel as the cycles of heating increased, indicating that the non-covalent interactions maintaining the cold gel were gradually disrupted. At higher dosage of TFE (42 and 56 μmol/g protein), cold induced gelation of DMP was inhibited at the beginning and gelation reversibility was also disappeared (Fig. 4).

3.3. Microstructure

The disparity in microstructures between thermally reversible DMP gel and TFE treated DMP gel was visualized by SEM. As displayed in Fig. 5A, DMP gels featured a homogeneous, and continuous gel matrix with smooth and compact cross-links. The porous network with closed cell morphology was visible throughout the gel matrix, which can be referred as a perforated lamellar structure. This belongs to a typical gel network formed by physical cross-links or entanglements. Similar percolating network topologies with thin connective walls and pores of varying size and spherical form were also discovered in thermally reversible gels of 2.5% pure gelatin (Treesuppharat et al., 2017) and 10% pea protein isolate (Zhu et al., 2022). In TFE treated DMP gel, uneven microstructures with thin lamellar connecting walls and irregular fragmentation were detected (Fig. 5B). TFE added DMP demonstrated macroscopic fluidity after heating but was unable to form an inversible gel upon cooling, and the overall solution was still homogeneous and had a slightly increased viscosity by cooling treatment (Fig. 3C). This suggests that there is still slight physical entanglements between DMP molecules during cooling even though TFE was included. It is probable that this physical entanglement will not allow the protein to form a firm and rigid gel network. The chain structure was unstable, and the interior structure disintegrated following lyophilization, resulting in an inhomogeneous microstructure with irregular edges (Fig. 5B). Overall, TFE addition prevented the formation of perforated lamellar structure in DMP.

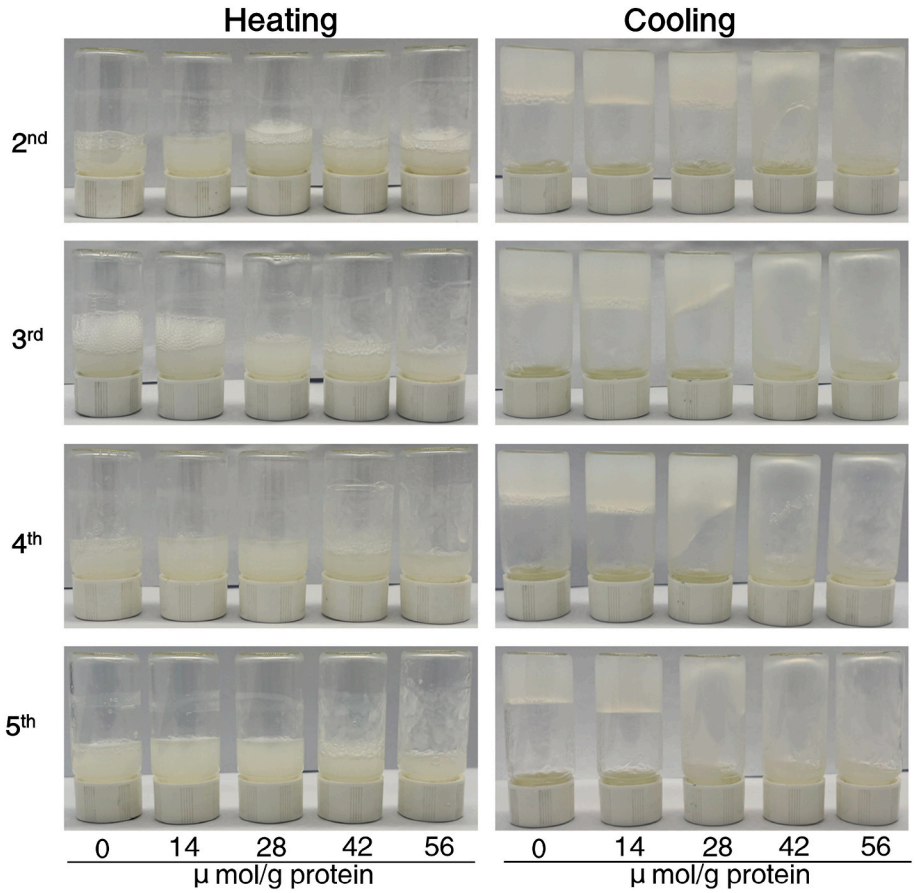

Fig. 4. Effects of TFE addition (0, 14, 28, 42, 56 μmol/g protein) on the gelation reversibility of DMP upon five cycles of heating and cooling.

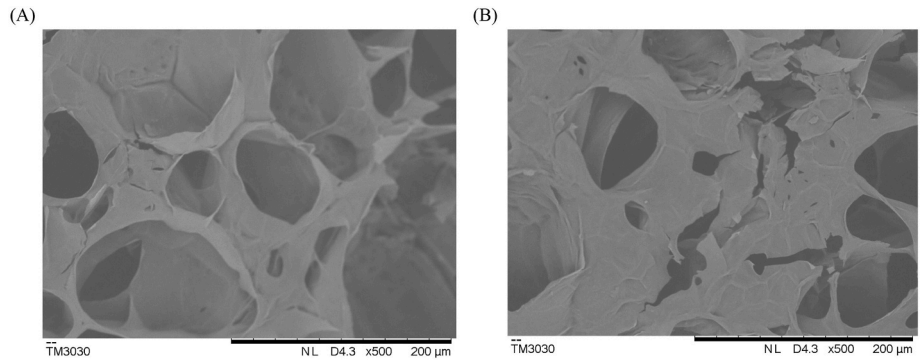

Fig. 5. Scanning electron microscopy images: (A) Freeze-dried sample after heating and cooling into gel by DMP; (B) The freeze-dried samples were heated and cooled by adding TFE (28 μmol/g protein) to DMP.

3.4. Rheological properties

The dynamic gelation behavior of DMP and TFE treated DMP was investigated using a time-temperature rheological profile tracked across two heating-cooling cycles (Fig. 6). During heating, DMP showed a characteristic rheological transition peak at around 53 °C, which has been attributed to the association of the myosin head. (Cao et al., 2016; Chen et al., 2019). G′ value exceptionally decreased upon heating beyond 53 °C. This was ascribed to the denaturation of light meromyosin, the dissociation of the actomyosin complex, and an increase in the 'fluidity' of the filaments (Chen et al., 2016a). This indicates that the DMP gel network is not established during the heating process. Deamidation produces more negative charges in myosin tails during heating, preventing myosin from performing tail-to-tail binding and, as a result, a decreased DMP's thermal gelation capacity (Fu et al., 2022; Xiong et al., 2010). The DMP solution gels on cooling and G′ rapidly increases, and the gel network can be disrupted on reheating, emerging in an instantaneous decrease in G′, while the gel can re-form upon re-cooling, resulting in a rebound in G′ on recooling, demonstrating typical thermally reversible gelation behavior. Presumably, the establishment of the DMP gel network is driven by reversible physical associations. The dynamic assembly of the myosin CC tails as described above mediated the formation of the gel network.

For the samples containing TFE, no establishment of the gel network was seen upon heating. The samples with TFE addition group exhibited a slight rise in G′ throughout the cooling stage, but no cold induced gel network was produced (Fig. 6). This is consistent with the macroscopic loss of gelation afore observed (Fig. 3C). The minor rise in G′ might be attributed to the slight cross-linking of myosin tails. The presence of TFE may prevent the formation of the cold gel network by inhibiting the assembly of α-helix into a convoluted helical structure as well as additional cross-linking (Othon et al., 2009). The rapid increase of G′ in the group with TFE addition during the secondary heating (Fig. 6) is attributed to the generation of some aggregates (they can be visualized in Fig. 4), which may be driven by covalent interactions as well as hydrogen bonding (Chen et al., 2018; Xiong et al., 2010). Subsequent heating maintenance can break the hydrogen bonds and cause molecular rearrangement (Zhu et al., 2022), leading to a sharp drop in G' (Fig. 6). In the second cooling stage, G′ showed a rebound which matches the fact that the sample solution presented an enhanced viscosity after second cooling. Based on the rheological results, it is seen that TFE diminished the gelation of DMP in the entire process of heating-cooling process, and DMP lost the thermally reversible gelation behavior with the addition of TFE. TFE effectively prevents the development of gel networks driven by reversible physical contacts (hydrophobic interactions) (Vymetal et al., 2016). We deduce that TFE operates primarily on the CC motif in the rod-like region of the myosin tail, inhibiting physical entanglement and dynamic assembly of the CC, eventually preventing the formation of thermally reversible cold gel network in DMP.

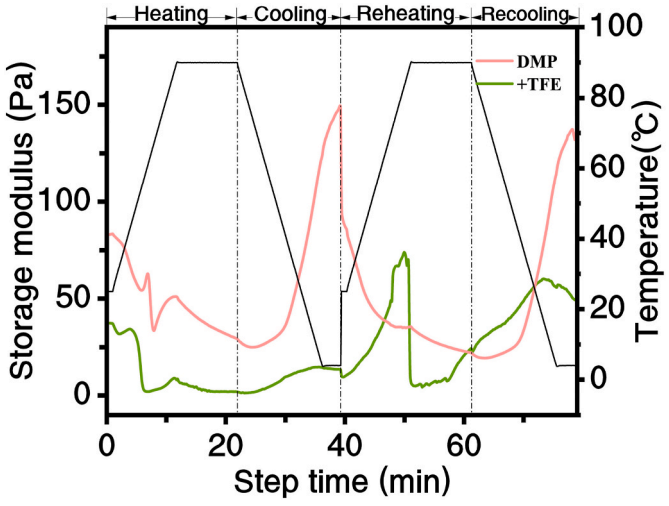

Fig. 6. Rheological curves of DMP and TEF added DMP within two heating and cooling cycles.

3.5. Secondary structure—α-helix

Two negative peaks were observed in the CD spectra of MPs between 208 and 222 nm, indicating the presence of α-helix in MPs (Fig. 7A). After the addition of TFE, the α-helix content is still prominent (Fig. 7A) with no significant changes. It suggests that TFE has no impacts on the overall secondary structure of DMP. Among them, the α-helix content remained the most abundant, which is consistent with previous report (Haider et al., 2018). Further calculations showed that the α-helix content varied with temperature as shown in Fig. 7B. The α-helix content of DMP decreased from 42.4% to 12.4% with increasing temperature. The significant loss of the α-helix indicates that the unfolding of helix and uncoiling of the CC of the myosin tail occurred during heating due to the disruption of hydrogen bonds (Chen et al., 2018; Liu and Xiong, 2015; Liu et al., 2008; Visessanguan et al., 2000). The preferential accumulation of TFE around the helix is probably the main reason why the α-helix structure is maintained in the protein, and the mechanism by which it promotes helix stability may be as follows: On the one hand, the presence of TFE disrupts the hydrogen bonding network and further reduces the entropic cost required for helix folding entropy. On the other hand, TFE may interfere with the protrusion of charged or highly polar side chains from the helix (Vymetal et al., 2016). During cooling, the α-helix content of the DMP showed a significant rebound, which was also persisted after the addition of TFE (Fig. 7B), indicating that TFE had no damaging effect on the secondary structure (α-helix) of the DMP. A similar conclusion was reached in a study on melittin

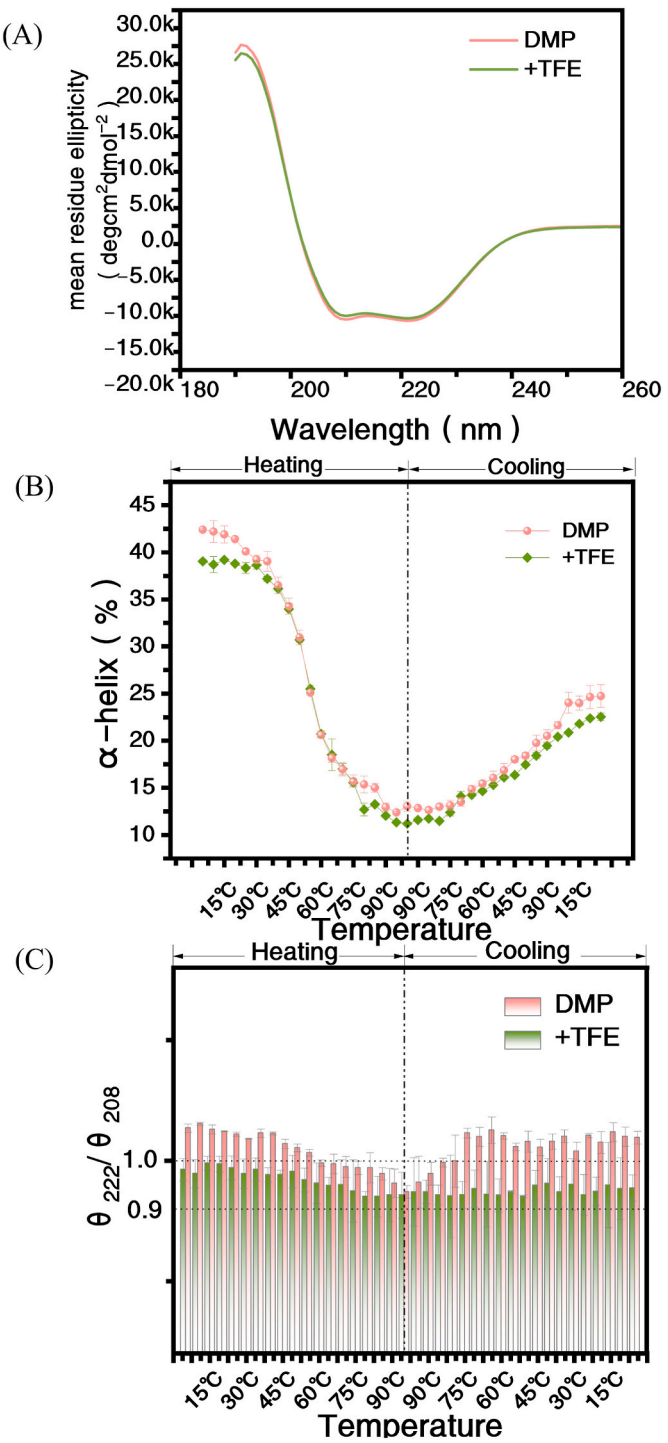

Fig. 7. Circular dichroism analysis of DMP and DMP added TFE. (A) Far-UV CD spectra; (B) α-helix contents and (C) $\theta_{222}/\theta_{208}$ during a temperature ramp of heating from 4 °C to 90 °C and cooling down to 4 °C.

tetramer-monomer, the inclusion of TFE modified the natural folding state of melittin, causing denaturation and stabilization of the monomeric helical structure while sustaining the helical secondary structure of the melittin (Othon et al., 2009).

3.6. Supramolecular structure—CC

CC is a vital building block for stimuli-responsive hydrogels due to its unique association-dissociation properties and specific spatial recognition capabilities, making it an ideal physically cross-linking motif for the construction of temperature-sensitive protein-based hydrogels (Fletcher et al., 2011; Olsen et al., 2010; Xu et al., 2005). The ratio $\theta_{222}/\theta_{208}$ is employed as a criterion for evaluating helical propensity (Choy et al., 2003). The ratio for a non-interacting α-helix is 0.9 (Hill et al., 2019), whereas the ratio for a two-stranded CC is 1.03 (Meleties et al., 2021; Zhou et al., 1992a; Zhou et al., 1992b). DMP is rich in filaments composed of a mass of myosin CC motifs (Zhang et al., 2022). The effect of DMP concentration on the $\theta_{222}/\theta_{208}$ ratio was firstly investigated to assess whether the formation of CC was the result of increasing protein concentration. The $\theta_{222}/\theta_{208}$ ratio was found to remain almost constant over the concentration range of 0.01 mg/mL to 0.2 mg/mL (Supplementary Fig. 1), indicating that the presence of CC was not associated with an increase in protein concentration.

The states of helical conformation responsive to temperature in DMP and DMP containing TFE were also monitored (Fig. 7C). As the heating process proceeds, the DMP undergoes a coil-to-helical transition ($\theta_{222}/\theta_{208}$ ratio decreased from ~1.05 to ~0.98) during heating, a conformational transition can be reversed on successive cooling, with the α-helix secondary structure reassembling into CC (as revealed by the $\theta_{222}/\theta_{208}$ ratio recovering back beyond 1.03), which was in line with previous studies (Zhang et al., 2022). By the addition of TFE, the $\theta_{222}/\theta_{208}$ radio of DMP decreased to 0.98 with heating but failed to rebound back to 1.03 upon subsequent cooling (Fig. 7C), indicating that the CC assembly in DMP was indeed inhibited probably due to the TFE jammed intermolecular association. TFE has an amphiphilic nature where the CF_3 group imparts significant hydrophobicity to the molecule and the electronegativity of fluorine increases the acidity of the OH group, rendering it an effective proton donor (Larzabal et al., 2019). These properties allow TFE to remain on the protein surface, displacing water molecules that would otherwise compete with intramolecular hydrogen bonds (Larzabal et al., 2019; Vymetal et al., 2016). The matrix of the TFE molecule can provide additional energy support through interactions with hydrophobic residues and weaken existing hydrophobic interactions, forcing the hydrophobic side chains into a relatively compact structure (Vymetal et al., 2016). Connecting with the macroscopic gel formation phenomenon (Fig. 3C), it can be concluded that the inhibition of the coiled helical structure prevents the formation of thermally reversible gels, and this reversely proofed that the assembly of the CC architecture is the key to the formation of thermally reversible gels of DMP.

The mechanism of thermally reversible gelation of DMP as affected by TFE are speculated in Fig. 8. After deamidation of PG, DMP contains many myosin-like filamentous structures at room temperature and when heated, the myosin head undergoes covalent aggregation and the tail unfolds (Zhang et al., 2022). During subsequent cooling, the oligomers undergo CC assembly on the helical tails via hydrophobic interactions. This results in a physically cross-linked gel network. However, for DMP with added TFE, the presence of the TFE prevents the assembly of the CC structure on cooling. Ultimately, this prevents the formation of thermally reversible gels and leaves the sample in a flowable suspension state.

4. Conclusion

The connection between CC structure and thermo-reversible gel formation was investigated using TFE. The results showed that TFE was able to specifically inhibit CC formation and protect the α-helix structure by disrupting hydrophobic interactions, under which the thermo-reversible gelation properties of DMP were lost, demonstrating that CC formation is the structural basis to thermo-reversible gelation of DMP. After deamidation, MP contains abundant filaments and a large number of myosin CC modules, these CC-based assemblies form a network of tangled fibrils that facilitate hydrogel formation during cooling which are responsible for cooling-induced gelation of DMP. These findings are intriguing as myosin CC can be targeted modified or

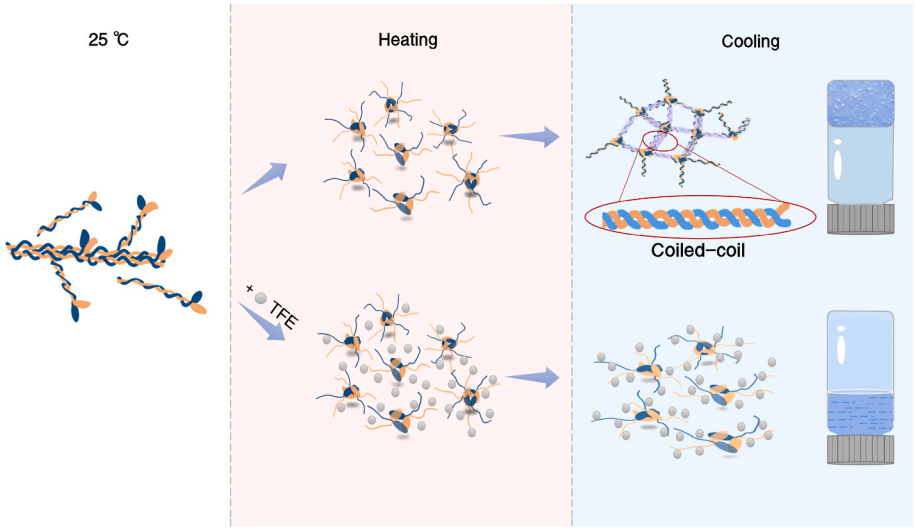

Fig. 8. Proposed mechanism of thermally reversible gelation of DMP as affected by TFE.

designed in the tailored manufacture of advanced meat products, for instance, the muscle protein gel or cultured meat products with temperature responsive mouthfeel. Additionally, this work underlines the use of TFE in deciphering the CC assembly in their stimuli-reversible gelation.

Funding sources

This work was financially supported by the Project funded by China Postdoctoral Science Foundation [grant number 2023M731336], National Natural Science Foundation of China [grant number 31901611], the Research Program of State Key Laboratory of Food Science and Resources, Jiangnan University [grant number SKLF-ZZA-202301] and Youth Talent Support Project of Jiangsu Association for Science and Technology [to Xing Chen].

CRediT authorship contribution statement

Lingying Zhang: Formal analysis, Data curation, Investigation, Visualization, and, Writing – original draft. **Yanna Zhang:** Data curation, Visualization, and, Writing – original draft. **Yue Wang:** Writing – review & editing. **Xing Chen:** Project administration, Conceptualization, Methodology, Software, Funding acquisition, Supervision, and, Writing – review & editing.

Declaration of competing interest

The authors declare that they have no known competing financial interests or personal relationships that could have appeared to influence the work reported in this paper.

Data availability

Data will be made available on request.

Acknowledgment

This work would like to acknowledge Peiqi Ni from Amano Enzyme Manufacturing Shanghai Branch for his assistance of protein glutaminase.

Appendix A. Supplementary data

Supplementary data to this article can be found online at https://doi.org/10.1016/j.crfs.2023.100611.

References

Aquinas, N., Bhat, M.R., Selvaraj, S., 2021. A review presenting production, characterization, and applications of biopolymer curdlan in food and pharmaceutical sectors. Polym. Bull. 79 (9), 6905–6927. https://doi.org/10.1007/s00289-021-03860-1.

Cao, Y., True, A.D., Chen, J., Xiong, Y.L., 2016. Dual role (anti- and pro-oxidant) of gallic acid in mediating myofibrillar protein gelation and gel in vitro digestion. J. Agric. Food Chem. 64 (15), 3054–3061. https://doi.org/10.1021/acs.jafc.6b00314.

Chen, X., Li, Y., Zhou, R.Y., Liu, Z.M., Lu, F.Z., Lin, H., Xu, X.L., Zhou, G.H., 2016a. L-histidine improves water retention of heat-induced gel of chicken breast myofibrillar proteins in low ionic strength solution. Int. J. Food Sci. Technol. 51 (5), 1195–1203. https://doi.org/10.1111/ijfs.13086.

Chen, X., Xiong, Y.L., Xu, X., 2019. High-pressure homogenization combined with sulfhydryl blockage by hydrogen peroxide enhance the thermal stability of chicken breast myofibrillar protein aqueous solution. Food Chem. 285, 31–38. https://doi.org/10.1016/j.foodchem.2019.01.131.

Chen, X., Xu, X.L., Liu, D.M., Zhou, G.H., Han, M.Y., Wang, P., 2018. Rheological behavior, conformational changes and interactions of water-soluble myofibrillar protein during heating. Food Hydrocolloids 77, 524–533. https://doi.org/10.1016/j.foodhyd.2017.10.030.

Chen, X., Xu, X.L., Zhou, G.H., 2016b. Potential of high pressure homogenization to solubilize chicken breast myofibrillar proteins in water. Innovat. Food Sci. Emerg. Technol. 33, 170–179. https://doi.org/10.1016/j.ifset.2015.11.012.

Choy, N., Raussens, V., Narayanaswami, V., 2003. Inter-molecular coiled-coil formation in human apolipoprotein E C-terminal domain. J. Mol. Biol. 334 (3), 527–539. https://doi.org/10.1016/j.jmb.2003.09.059.

Dexter, A.F., Fletcher, N.L., Creasey, R.G., Filardo, F., Boehm, M.W., Jack, K.S., 2017. Fabrication and characterization of hydrogels formed from designer coiled-coil fibril-forming peptides. RSC Adv. 7 (44), 27260–27271. https://doi.org/10.1039/c7ra02811c.

Dong, H., Paramonov, S.E., Hartgerink, J., 2008. Self-assembly of α-helical coiled-coil nanofibers. J. Am. Chem. Soc. 130 (41), 13691–13695. https://doi.org/10.1021/ja8037323.

Du, L., Brenner, T., Xie, J.L., Matsukawa, S., 2016. A study on phase separation behavior in kappa/iota carrageenan mixtures by micro DSC, rheological measurements and simulating water and cations migration between phases. Food Hydrocolloids 55, 81–88. https://doi.org/10.1016/j.foodhyd.2015.11.004.

Fletcher, N.L., Lockett, C.V., Dexter, A.F., 2011. A pH-responsive coiled-coil peptide hydrogel. Soft Matter 7 (21), 10210–10218. https://doi.org/10.1039/c1sm06261a.

Fu, W.Y., Chen, X., Cheng, H., Liang, L., 2022. Tailoring protein intrinsic charge by enzymatic deamidation for solubilizing chicken breast myofibrillar protein in water. Food Chem. 385, 132512 https://doi.org/10.1016/j.foodchem.2022.132512.

Gong, H.H., Liu, J., Wang, L.M., You, L., Yang, K., Ma, J., Sun, W.Q., 2022. Strategies to optimize the structural and functional properties of myofibrillar proteins: physical and biochemical perspectives. Crit. Rev. Food Sci. Nutr. 1–17. https://doi.org/10.1080/10408398.2022.2139660.

Gunasekar, S.K., Asnani, M., Limbad, C., Haghpanah, J.S., Hom, W., Barra, H., Nanda, S., Lu, M., Montclare, J.K., 2009. N-terminal aliphatic residues dictate the structure, stability, assembly, and small molecule binding of the coiled-coil region of cartilage oligomeric matrix protein. Biochemistry 48 (36), 8559–8567. https://doi.org/10.1021/bi900534r.

Guo, M., Mei, Y., 2013. Equilibrium and folding simulations of NS_4B H_2 in pure water and water/2,2,2-trifluoroethanol mixed solvent: examination of solvation models. J. Mol. Model. 19 (9), 3931–3939. https://doi.org/10.1007/s00894-013-1933-6.

Haider, M.J., Zhang, H.V., Sinha, N., Fagan, J.A., Kiick, K.L., Saven, J.G., Pochan, D.J., 2018. Self-assembly and soluble aggregate behavior of computationally designed coiled-coil peptide bundles. Soft Matter 14 (26), 5488–5496. https://doi.org/10.1039/c8sm00435h.

Hayakawa, F., Kazami, Y., Ishihara, S., Nakao, S., Nakauma, M., Funami, T., Nishinari, K., Kohyama, K., 2014. Characterization of eating difficulty by sensory evaluation of hydrocolloid gels. Food Hydrocolloids 38, 95–103. https://doi.org/10.1016/j.foodhyd.2013.11.007.

Hill, L.K., Meleties, M., Katyal, P., Xie, X., Delgado-Fukushima, E., Jihad, T., Liu, C.F., O'Neill, S., Tu, R.S., Renfrew, P.D., Bonneau, R., Wadghiri, Y.Z., Montclare, J.K., 2019. Thermoresponsive protein-engineered coiled-coil hydrogel for sustained small molecule release. Biomacromolecules 20 (9), 3340–3351. https://doi.org/10.1021/acs.biomac.9b00107.

Ito, Y., Tatsumi, y., Wakamatsu, J.I., Nishimura, T., Hattori, A., 2003. The solubilization of myofibrillar proteins of vertebrate skeletal muscle in water. Anim. Sci. J. 74 (5), 417–425. https://doi.org/10.1046/j.1344-3941.2003.00134.x.

Khan, T., Park, J.K., Kwon, J.H., 2007. Functional biopolymers produced by biochemical technology considering applications in food engineering. Kor. J. Chem. Eng. 24 (5), 816–826. https://doi.org/10.1007/s11814-007-0047-1.

Larzabal, M., Baldoni, H.A., Suvire, F.D., Curto, L.M., Gomez, G.E., Da Silva, W.M., Giudicessi, S.L., Camperi, S.A., Delfino, J.M., Cataldi, A.A., Enriz, D., 2019. An inhibitory mechanism of action of coiled-coil peptides against type three secretion system from enteropathogenic Escherichia coli. J. Pept. Sci. 25 (3), e3149. https://doi.org/10.1002/psc.3149.

Li, N., Liu, C.J., Chen, W., 2019. Facile access to guar gum based supramolecular hydrogels with rapid self-healing ability and multistimuli responsive gel-sol transitions. J. Agric. Food Chem. 67 (2), 746–752. https://doi.org/10.1021/acs.jafc.8b05130.

Liu, C., Xiong, Y.L., 2015. Oxidation-initiated myosin subfragment cross-linking and structural instability differences between white and red muscle fiber types. J. Food Sci. 80 (1–3), C288–C297. https://doi.org/10.1111/1750-3841.12749.

Liu, H.T., Zhang, H., Liu, Q., Chen, Q., Kong, B.H., 2021. Filamentous myosin in low-ionic strength meat protein processing media: assembly mechanism, impact on protein functionality, and inhibition strategies. Trends Food Sci. Technol. 112, 25–35. https://doi.org/10.1016/j.tifs.2021.03.039.

Liu, R., Zhao, S.M., Xiong, S.B., Xie, B.J., Qin, L.H., 2008. Role of secondary structures in the gelation of porcine myosin at different pH values. Meat Sci. 80 (3), 632–639. https://doi.org/10.1016/j.meatsci.2008.02.014.

Liu, X., Billington, N., Shu, S., Yu, S.H., Piszczek, G., Sellers, J.R., Korn, E.D., 2017. Effect of ATP and regulatory light-chain phosphorylation on the polymerization of mammalian nonmuscle myosin II. Proc. Natl. Acad. Sci. USA 114 (32), E6516–E6525. https://doi.org/10.1073/pnas.1702375114.

Meleties, M., Katyal, P., Lin, B., Britton, D., Montclare, J.K., 2021. Self-assembly of stimuli-responsive coiled-coil fibrous hydrogels. Soft Matter 17 (26), 6470–6476. https://doi.org/10.1039/d1sm00780g.

Nitta, Y., 2023. Study of polysaccharide gels at Prof. Nishinari's laboratory. Food Hydrocolloids 136, 108256. https://doi.org/10.1016/j.foodhyd.2022.108256.

Olsen, B.D., Kornfield, J.A., Tirrell, D.A., 2010. Yielding behavior in injectable hydrogels from telechelic proteins. Macromolecules 43 (21), 9094–9099. https://doi.org/10.1021/ma101434a.

Othon, C.M., Kwon, O.H., Lin, M.M., Zewail, A.H., 2009. Solvation in protein (un)folding of melittin tetramer-monomer transition. Proc. Natl. Acad. Sci. USA 106 (31), 12593–12598. https://doi.org/10.1073/pnas.0905967106.

Prince, E., Kumacheva, E., 2019. Design and applications of man-made biomimetic fibrillar hydrogels. Nat. Rev. Mater. 4 (2), 99–115. https://doi.org/10.1038/s41578-018-0077-9.

Rahmani, H., Ma, W., Hu, Z., Daneshparvar, N., Taylor, D.W., McCammon, J.A., Irving, T.C., Edwards, R.J., Taylor, K.A., 2021. The myosin II coiled-coil domain atomic structure in its native environment. Proc. Natl. Acad. Sci. U.S.A. 118 (14), e2024151118 https://doi.org/10.1073/pnas.2024151118.

Sala, G., Stieger, M., van de Velde, F., 2010. Serum release boosts sweetness intensity in gels. Food Hydrocolloids 24 (5), 494–501. https://doi.org/10.1016/j.foodhyd.2009.12.001.

Treesuppharat, W., Rojanapanthu, P., Siangsanoh, C., Manuspiya, H., Ummartyotin, S., 2017. Synthesis and characterization of bacterial cellulose and gelatin-based hydrogel composites for drug-delivery systems. Biotechnol. Rep. 15, 84–91. https://doi.org/10.1016/j.btre.2017.07.002.

Tunn, I., 2020. From single molecules to bulk materials: tuning the viscoelastic properties of coiled coil cross-linked hydrogels. Universität Potsdam. https://doi.org/10.25932/publishup-47595.

Visessanguan, W., Ogawa, M., Nakai, S., An, H., 2000. Physicochemical changes and mechanism of heat-induced gelation of arrowtooth flounder myosin. J. Agric. Food Chem. 48 (4), 1016–1023. https://doi.org/10.1021/jf9900332.

Vymetal, J., Bednarova, L., Vondrasek, J., 2016. Effect of TFE on the helical content of AK17 and HAL-1 peptides: theoretical insights into the mechanism of helix stabilization. J. Phys. Chem. B 120 (6), 1048–1059. https://doi.org/10.1021/acs.jpcb.5b11228.

Wang, H.Y., Heilshorn, S.C., 2015. Adaptable hydrogel networks with reversible linkages for tissue engineering. Adv. Mater. 27 (25), 3717–3736. https://doi.org/10.1002/adma.201501558.

Wang, Y., Katyal, P., Montclare, J.K., 2019. Protein-engineered functional materials. Adv. Healthcare Mater. 8 (11), e1801374 https://doi.org/10.1002/adhm.201801374.

Wang, Y.C., Wang, R., Chang, Y.G., Gao, Y., Li, Z.J., Xue, C.H., 2015. Preparation and thermo-reversible gelling properties of protein isolate from defatted Antarctic krill (Euphausia superba) byproducts. Food Chem. 188, 170–176. https://doi.org/10.1016/j.foodchem.2015.04.126.

Xiong, Y.L., Blanchard, S.P., Ooizumi, T., Ma, Y., 2010. Hydroxyl radical and ferryl-generating systems promote gel network formation of myofibrillar protein. J. Food Sci. 75 (2), C215–C221. https://doi.org/10.1111/j.1750-3841.2009.01511.x.

Xu, C.Y., Breedveld, V., Kopeček, J.i., 2005. Reversible hydrogels from self-assembling genetically engineered protein block copolymers. Biomacromolecules 6 (3), 1739–1749. https://doi.org/10.1021/bm050017f.

Yan, H., Nykanen, A., Ruokolainen, J., Farrar, D., Gough, J.E., Saiani, A., Miller, A.F., 2008. Thermo-reversible protein fibrillar hydrogels as cell scaffolds. Faraday Discuss 139, 71–84. https://doi.org/10.1039/b717748h.

Yoshikawa, Y., Yasuike, T., Yagi, A., Yamada, T., 1999. Transverse elasticity of myofibrils of rabbit skeletal muscle studied by atomic force microscopy. Biochem. Biophys. Res. Commun. 256 (1), 13–19. https://doi.org/10.1006/bbrc.1999.0279.

Yu, Y.B., 2002. Coiled-coils: stability, specificity, and drug delivery potential. Adv. Drug Deliv. Rev. 54, 1113–1129. https://doi.org/10.1016/S0169-409X(02)00058-3.

Zhang, L.Y., Chen, X., Wang, Y., Xu, X.L., Zhou, P., 2022. Myofibrillar protein can form a thermo-reversible gel through elaborate deamidation using protein-glutaminase. J. Sci. Food Agric. 103 (6), 3118–3128. https://doi.org/10.1002/jsfa.12287.

Zhou, X., Niu, L.H., Bai, Y., Huang, Y.Q., Lei, K.Q., Wang, Y., 2012. Effect of different acid treatment on yield and physicochemical properties of gelatin derived from tilapia skin. J. Food Sci. Technol. 30 (2), 22–26. https://doi.org/10.3969/j.issn.2095-6002.2012.02.005.

Zhou, N.E., Kay, C.M., Hodges, R.S., 1992a. Synthetic model proteins the relative contribution of leucine residues at the nonequivalent positions of the 3-4 hydrophobic repeat to the stability of the two-stranded .alpha.-helical coiled-coil. Biochemistry 31 (25), 5739–5746. https://doi.org/10.1021/bi00140a008.

Zhou, N.E., Zhu, B.Y., Kay, C.M., Hodges, R.S., 1992b. The two-stranded α-helical coiled-coil is an ideal model for studying protein stability. Biopolymers 32 (4), 419–426. https://doi.org/10.1002/bip.360320419.

Zhu, P.N., Huang, W.J., Chen, L.Y., 2022. Develop and characterize thermally reversible transparent gels from pea protein isolate and study the gel formation mechanisms. Food Hydrocolloids 125. https://doi.org/10.1016/j.foodhyd.2021.107373.